JPET Fast Forward. Published on March 28, 2017 as DOI: 10.1124/jpet.117.240184
This article has not been copyedited and formatted. The final version may differ from this version.

Title Page

Pharmaceutical characterization of tropomyosin receptor kinase B-agonistic antibodies on human iPS cell-derived neurons

Stefanie Traub, Heiko Stahl, Holger Rosenbrock, Eric Simon, Lore Florin, Lisa Hospach, Stefan Hörer, Ralf Heilker

Trenzyme GmbH (S.T.), Byk-Gulden –Str. 2, D-78467 Konstanz, Germany; Lead Identification and Optimization Support (L.H., S.H., R.H.), Immunological and Respiratory Diseases Research (H.S.), CNS Diseases Research (H.R.), Target Discovery Research (E.S.); Boehringer Ingelheim Pharma GmbH & Co. KG, Birkendorfer Str. 65, D-88397 Biberach, Germany; Biotherapeutics Discovery (L.F.); Boehringer Ingelheim Pharmaceuticals Inc., 900 Ridgebury Road, Ridgefield, CT 06877, USA

Primary laboratory of origin:

Dr. Ralf Heilker

Boehringer Ingelheim Pharma GmbH & Co. KG

Lead Identification and Optimization Support

Birkendorfer Straße 65

D-88397 Biberach an der Riss

phone +49-7351-54 5590

fax +49-7351-83 5590

email Ralf.Heilker@boehringer-ingelheim.com

Running Title Page

Running title: TrkB-agonistic antibodies on human iPS cell-derived neurons

Corresponding author:

Dr. Ralf Heilker

Boehringer Ingelheim Pharma GmbH & Co. KG

Lead Identification and Optimization Support

Birkendorfer Straße 65

D-88397 Biberach an der Riss

phone +49-7351-54 5590

fax +49-7351-83 5590

email Ralf.Heilker@boehringer-ingelheim.com

Number of text pages: 40

Number of tables: 1

Number of figures: 6

Number of references: 22

Number of words in the *Abstract*: 250

Number of words in the *Introduction*: 507

Number of words in the *Discussion*: 1633

Recommended section assignment: Neuropharmacology

ABBREVIATIONS: AKT kinase, Ak strain thymoma kinase; BDNF, Brain-derived neurotrophic factor; CHO, Chinese Hamster Ovary; CREB, cAMP response element-binding protein; ERK, extracellular-signal regulated kinase; hiPS cells, human induced pluripotent stem cells; NGF, Nerve growth factor; NGS, next generation sequencing; NT, neurotrophin; Trk, tropomyosin receptor kinase.

JPET Fast Forward. Published on March 28, 2017 as DOI: 10.1124/jpet.117.240184
This article has not been copyedited and formatted. The final version may differ from this version.

Abstract

Brain-derived neurotrophic factor (BDNF) is a central modulator of neuronal development and synaptic plasticity in the central nervous system (CNS). This renders the BDNF-modulated tropomyosin receptor kinase B (TrkB) a promising drug target to treat synaptic dysfunctions. Using GRowth factor-driven expansion and INhibition of NotCH during maturation, the so-called GRINCH neurons were derived from human induced pluripotent stem (hiPS) cells. These GRINCH neurons were employed as model cells for pharmacological profiling of two TrkB-agonistic antibodies, hereafter referred to as AB2 and AB20. In next generation sequencing (NGS) studies, AB2 and AB20 stimulated transcriptional changes, which extensively overlapped with BDNF-driven transcriptional modulation. In regard to TrkB phosphorylation, both AB2 and AB20 were only about half as efficacious as BDNF. However, with respect to the TrkB downstream signaling, AB2 and AB20 displayed increased efficacy values, providing a stimulation at least comparable to BDNF in respect of *VGF* transcription as well as of AKT and CREB phosphorylation. In a complex structure of the TrkB-d5 domain with AB20, determined by x-ray crystallography, the AB20 binding site was found to be allosteric in regard to the BDNF binding site while AB2 was known to act orthosterically with BDNF. In agreement with this finding, AB2 and AB20 acted synergistically at higher concentrations to drive TrkB phosphorylation. Whilst TrkB downstream signaling declined faster after pulse stimulation with AB20 than with AB2, AB20 restimulated TrkB phosphorylation more efficiently than AB2. In conclusion, both antibodies displayed some limitations and some benefits in regard to future applications as therapeutic agents.

Introduction

Nerve growth factor (NGF), BDNF (Barde et al., 1982), neurotrophin-3 (NT3) and neurotrophin-4 (NT4) represent the neurotrophin family of growth factors, acting upon TrkA, TrkB, TrkC and p75 neurotrophin receptor (Bothwell, 2014). While all four neurotrophins are agonists for p75NTR, they display some selectivity in regard to the Trk receptors: NGF is a preferential agonist for TrkA, NT3 for TrkC, BDNF and NT4 for TrkB (Bothwell, 2014). Among the neurotrophins, BDNF stands out for its high expression levels in the CNS and its effects on synaptic plasticity (Adachi et al., 2014). Accordingly, BDNF has been implicated in a multitude of CNS-related diseases (Adachi et al., 2014) such as Alzheimer's disease, Parkinson's disease, schizophrenia, depression, bipolar disorder, anxiety, Huntington's disease, stroke, epilepsy, eating disorders, and substance use.

Therefore, pharmacological stimulation of TrkB holds the potential for the treatment of various CNS disorders (Longo and Massa, 2013). However, the dimensions of the BDNF dimer and its cognate binding sites on TrkB are beyond what can typically be bridged by a small molecule (Longo and Massa, 2013). Yet, since there are possibilities (Pardridge, 2012) to shuttle a new biological entity (NBE) across the blood brain barrier (BBB), a bivalent biopharmaceutical agent such as an agonistic antibody against TrkB could drive receptor dimerization and its transphosphorylation in a similar manner as the dimeric physiological TrkB agonist BDNF. Accordingly, two antibodies AB2 and AB20 (Lin et al., 2010; Wang et al., 2010) directed against extracellular epitopes of TrkB have been analyzed in this work.

In regard to the ultimate target cells of biopharmaceutical TrkB modulators, an ideal *in vitro* model system would employ human neurons. Such cells express TrkB and downstream signaling components in physiological amounts and correct

JPET Fast Forward. Published on March 28, 2017 as DOI: 10.1124/jpet.117.240184
This article has not been copyedited and formatted. The final version may differ from this version.

stoichiometric ratios. While the access to primary human neurons is obviously rather limited, the advent of hiPS cell technology has enabled the differentiation towards neuronal target cells in huge numbers, for instance, the so-called GRINCH neurons (Heilker et al., 2014; Traub et al., 2017).

While the endogenous expression levels of TrkB and TrkB-associated signaling biomolecules in GRINCH neurons represent a better physiological recapitulation of the *in vivo* systems, it is much more challenging to measure the respective pharmacological responses than in a recombinant system. To address this challenge, the highly sensitive amplified luminescent proximity homogeneous assay LISA (AlphaLISA) format (Cauchon et al., 2009) and an HTS-adapted version of Reverse Transcription-Polymerase Chain Reaction (RT-PCR) were employed (Traub et al., 2017).

For the pharmacological profiling of drug candidates, it is very important to monitor one of the disease-relevant signaling events associated with the drug target (Heilker et al., 2014). In this work, we compared the efficacies of BDNF, AB2 and AB20 in regard to (i) TrkB phosphorylation, (ii) TrkB downstream signaling modulators ERK, AKT and CREB as well as (iii) the TrkB-driven transcription of the synaptic plasticity marker *VGF* mRNA as an early response gene (Alder et al., 2003). Thus, the applied experimental profiling panel monitors drug efficacy check-points all along the signaling chain from the drug target TrkB towards *VGF* as a disease-relevant biomarker end-point.

JPET Fast Forward. Published on March 28, 2017 as DOI: 10.1124/jpet.117.240184
This article has not been copyedited and formatted. The final version may differ from this version.

Methods

BDNF and agonistic antibodies

BDNF was purchased from Biotrend Chemikalien GmbH (Cologne, Germany; cat# CYT-207; molecular weight of 26,984 Da for the homodimer). AB2 was derived from the previously described antibody C2 (Lin et al., 2010). In AB2, the humanized V-regions of C2 were grafted onto the constant regions of a human immunoglobulin (Ig) G1 antibody. AB20 was derived from the previously described antibody C20 (Wang et al., 2010), by grafting the murine V-regions of C20 onto the constant regions of a human IgG1 antibody. Isotype-matched control anti-2,4,6 trinitrophenyl (TNP) antibody (IgG, derived from 1B7.11; American Type Culture Collection, Rockville, MD) was used as reference. Fc-mediated effector functions of all antibodies were reduced by mutating leucines 234 and 235 to alanines (Xu et al., 2000).

Human iPS cell maintenance culture and neuronal differentiation

The minicircle hiPS cell line (catalogue number [cat#] SC301A-1) was purchased from System Biosciences (Mountain View, CA). Human iPS cell maintenance culture, neural induction, neural progenitor (NP) cell expansion, and final neuronal differentiation towards GRINCH neurons were carried out as described previously.

CellSensor™ cell lines

CellSensor™ Chinese Hamster Ovary K1 (CHO-K1) cell lines, which are stably co-transfected with (i) a gene encoding a nuclear factor of activated T-cells (NFAT) promoter-regulated beta lactamase reporter and (ii) a gene encoding TrkA (cat#

JPET Fast Forward. Published on March 28, 2017 as DOI: 10.1124/jpet.117.240184
This article has not been copyedited and formatted. The final version may differ from this version.

K1516), TrkB (cat# K1491), or TrkC (cat# K1491), were purchased from Life Technologies (Carlsbad, CA). The three cell lines will further be referred to as "CHO-TrkA/B/C" cells, respectively. The cells were cultured according to manufacturer's instructions. For the below described 384-well Alpha™ assays and immunofluorescence staining, the cells were seeded at a concentration of 100,000 cells/cm² into one well of a black PureCoat™ amine-coated 384-well plate (cat# 359324; Corning Inc., Corning, NY), and cultured for 24 h.

Next generation sequencing (NGS)

NGS was carried out as described in the Supplement.

RT-PCR from non-purified cellular lysate

Stimulation of TrkB signaling for the RT-PCR format

The supernatant of the 384-well microplates containing the 6,000 GRINCH neurons/well (hereafter referred to as the "cell plate") was aspirated to a residual volume of 10 µL/well using a BioTek EL406 Washer Dispenser. Stimulation buffer consisted of 1x Dulbecco's phosphate buffered saline (DPBS), supplemented with 1% (w/v) bovine serum albumin (BSA; cat# A3059-100g, Sigma-Aldrich, St. Louis, MO). An equal volume of 10 µL/well of stimulation buffer containing BDNF, AB2, AB20 or IgG control was added to the cellular supernatant producing the indicated final concentrations. The cells were then incubated for 6 h at 37°C and 5% CO_2.

For pathway inhibition experiments, 10 µL/well of 20 µM K252a, 100 µM PD98059, 50 µM LY294002 or 100 µM U73122 diluted in stimulation buffer supplemented with

JPET Fast Forward. Published on March 28, 2017 as DOI: 10.1124/jpet.117.240184
This article has not been copyedited and formatted. The final version may differ from this version.

2 % DMSO, were added to the cellular supernatant prior to agonist addition. After incubating for 30 min at 37°C and 5% CO_2 with one of the above small molecule inhibitors, 20 µL/well of the indicated agonist diluted in stimulation buffer was added resulting in final concentrations of 100 ng/mL BDNF (3.7 nM), 100 ng/mL AB2 (0.66 µM), 100 ng/mL AB20 (0.66 µM). The cells were then incubated for 6 h at 37°C and 5% CO_2.

Cell lysis and VGF gene expression measurement in the RT-PCR format

After the above described 6 h of stimulation, the GRINCH neurons were washed three times with 70 µL/well 1x DPBS, and the supernatant was aspirated to a residual volume of 10 µL/well using a BioTek EL406 Washer Dispenser. Subsequently, the cells were lysed for 5 min at room temperature using 10 µL/well 1x Realtime Ready Cell Lysis Buffer, supplemented with 2x RNase inhibitor (Realtime Ready Cell Lysis Kit, cat# 05943523001, Roche, Basel, Switzerland). Next, 9 µL/well Realtime ready master mix, composed of 1x Realtime Ready virus master (cat# 05992877001, Roche) and 1x Realtime Ready Catalogue (cat# 05532957001, Roche) primer probe set for *VGF* (Assay ID: 146837) was prepared and transferred into a 384-well LightCycler™ 480 plate (cat# 04729749001, Roche). Then 1 µL/well of the lysate was transferred from the cell plate to the 384-well LightCycler™ 480 plate, using the CyBi™-Well vario 384 Channel Simultaneous Pipettor (Cybio, Jena, Germany). The LightCycler™ 480 plate was sealed and centrifuged for 4 min at 1,500 g. Gene expression was measured using a LightCycler™ 480 instrument. The following RT-PCR program was used: (1) Reverse Transcription: 50°C, 8 min, 1 cycle; (2) Pre-incubation: 95°C, 30 s, 1 cycle; (3) Amplification: 95°C, 1 s, followed by 60°C, 20 s, 45 cycles; (4) Cooling: 40°C, 30 s, 1 cycle.

AlphaLISA format

Stimulation of TrkB signaling for the AlphaLISA format

The supernatant of the 384-well microplates containing the 6,000 GRINCH neurons/well or 10,000 CHO-TrkA/B/C cells/well (hereafter referred to as the "cell plate") was aspirated to a residual volume of 10 µL/well using a BioTek EL406 Washer Dispenser. An equal volume of 10 µL/well of BDNF, AB2, AB20 or IgG control in stimulation buffer was added for 15 min at 37°C and 5% CO_2 resulting in the respectively indicated concentrations of agonists. For synergism experiments, the GRINCH neurons were stimulated for 15 min at 37°C and 5% CO_2 with combinations of BDNF and AB2, BDNF and AB20, or AB2 and AB20 at the indicated concentrations.

For pathway inhibition experiments, 10 µL/well of 20 µM K252a, 100 µM PD98059, 50 µM LY294002 or 100 µM U73122 diluted in stimulation buffer, were added to the cellular supernatant prior to agonist addition. After incubating for 30 min at 37°C and 5% CO_2 with one of the above small molecule inhibitors, 20 µL/well of the indicated agonist diluted in stimulation buffer was added resulting in final concentrations of 100 ng/mL BDNF (3.7 nM), 100 ng/mL AB2 (0.66 µM), 100 ng/mL AB20 (0.66 µM). The cells were then incubated for 15 min at 37°C and 5% CO_2.

In order to analyze the kinetics of TrkB signaling pathways after stimulation with BDNF, AB2 or AB20, three different stimulation schemes were applied. All incubations were carried out at 37°C and 5% CO_2. For the "re-stimulation" scheme, the GRINCH neurons were stimulated for 15 min with 10 ng/mL BDNF (0.37 nM), 100 ng/mL AB2 (0.66 µM) or 1 µg/mL AB20 (6.67 µM) in stimulation buffer, then washed three times with 70 µL/well neural differentiation medium (Traub et al., 2017),

JPET Fast Forward. Published on March 28, 2017 as DOI: 10.1124/jpet.117.240184
This article has not been copyedited and formatted. The final version may differ from this version.

incubated for the indicated variable intermittent phase in the absence of an agonist, and subsequently stimulated again for 15 min until cellular lysis with the same concentrations of BDNF, AB2, AB20 as administered prior to the intermittent phase. For the “single pulse” scheme, the GRINCH neurons were stimulated for 15 min with 10 ng/mL BDNF (0.37 nM), 100 ng/mL AB2 (0.66 µM) or 1 µg/mL AB20 (6.67 µM) in stimulation buffer, then washed three times with 70 µL/well neural differentiation medium, incubated for the indicated variable time period in the absence of an agonist. For the “continuous stimulation” scheme, the GRINCH neurons were stimulated for the indicated variable time period with 10 ng/mL BDNF (0.37 nM), 100 ng/mL AB2 (0.66 µM) or 1 µg/mL AB20 (6.67 µM).

Cell lysis

After stimulation, GRINCH neurons or CHO-TrkA/B/C cells were washed three times with 70 µL/well 1x DPBS, and the supernatant was aspirated off to a residual volume of 10 µL/ well using a BioTek EL406 Washer Dispenser. Subsequently, the cells were lysed for 5 min at room temperature by addition of 10 µL/well 1x CST lysis buffer (cat# 9803, Cell Signaling Technology, Danvers, MA), supplemented with 2x Protease inhibitor (cat# 11873580001, Roche) and 2x Phosphatase inhibitor cocktails 2 and 3 (cat# P5726, cat# P0044, Sigma-Aldrich).

Trk phosphorylation measured in the Alpha™ format

Custom-made Alpha™ reagents were employed to measure Trk phosphorylation: AlphaLISA™ Acceptor beads (cat# 6772003, PerkinElmer, Hopkinton, MA) were

JPET Fast Forward. Published on March 28, 2017 as DOI: 10.1124/jpet.117.240184
This article has not been copyedited and formatted. The final version may differ from this version.

conjugated with an anti-phosphorylated Trk (pTrk) antibody (cat# 4621BF, Cell Signaling Technology), which non-selectively detects TrkA, TrkB or TrkC phosphorylated at the tyrosine, homologous to Tyr706 in TrkB. (i) For the selective detection of phosphorylated TrkB (pTrkB), the above prepared Acceptor beads were used together with a biotinylated, isoform-selective anti-TrkB antibody (cat# MAB3971, R&D Systems Inc., Minneapolis, MN) and streptavidin-coated Alpha™ Donor beads (cat# 6760002B, PerkinElmer). (ii) For the non-selective detection of all three phosphorylated Trk isoforms, the above prepared Acceptor beads were used together with a biotinylated, anti-pan-Trk antibody (cat# 4609BF, Cell Signaling Technology) and streptavidin-coated Alpha™ Donor beads.

Using these Alpha™ reagents, 5 µL/well of the above produced cellular lysate were transferred into the corresponding well of a 384-well small volume flat bottom plate (cat# 784075, Greiner Bio-One GmbH, Frickenhausen, Germany) for Alpha™ detection using a CyBi™-Well vario 384 Channel Simultaneous Pipettor. Subsequently, 2.5 µL/well of the anti-pTrk Acceptor beads (final concentration: 10 µg/mL), diluted in 1x AlphaLISA™ Assay buffer (cat# AL000F, PerkinElmer) were added. The microplate was incubated for 45 min at room temperature. Subsequently, 2.5 µL/well of the respective biotinylated antibody (final concentration: 1 nM, diluted in 1x AlphaLISA™ Assay buffer) were added. The microplate was incubated for 45 min at room temperature. Finally, 2.5 µL/well of Alpha™ streptavidin-coated donor beads (final concentration: 20 µg/mL, diluted in 1x AlphaLISA™ Assay buffer) were added under subdued light conditions. The microplate was incubated for 30 min at room temperature in the dark. The AlphaLISA™ signal was measured using an Envision Reader (extinction: 680 nm/ emission: 615 nm) purchased from PerkinElmer.

Phosphorylation of ERK, AKT, or CREB measured in the Alpha^{TM} format

For the detection of ERK, AKT, and CREB phosphorylation, AlphaScreen™ Surefire™ kits for pERK 1/2 (Thr202/Tyr204; cat# TGRES50K, PerkinElmer), pAKT 1/2/3 (Ser473; cat# TGRA4S50K, PerkinElmer) and pCREB (Ser133; cat# TGRCBS50K, PerkinElmer) were used with the above generated cellular lysates according to the manufacturer's instructions.

Immunofluorescence staining of CHO-TrkA/B/C lines

The CHO-TrkA/B/C cells were stimulated for 15 min at 37°C and 95% CO_2 with 10 µg/mL AB2 or AB20. Subsequently, the cells were washed three times with 1x Tris Buffered Saline (TBS; cat# T5912-1L, Sigma-Aldrich) and then fixed with 4% (v/v) paraformaldehyde solution (cat# 252549-500ml, Sigma-Aldrich) for 15 min at room temperature. Next, the cells were washed three times with 1x TBS and were incubated with 10% (v/v) Fetal Bovine Serum (FBS, cat# 26140-079, Life Technologies) in 1x TBS for 60 min at room temperature. The cells were then washed three times with 1x TBS, and were incubated with species-specific secondary Alexa Fluor^{TM} antibodies (Thermo Fisher Scientific Inc., Waltham, MA) diluted in 1x TBS at room temperature for 2 h in the dark. Finally, the cells were washed once with 1x TBS, incubated for 5 min with 300 µM 4′,6-Diamidin-2-phenylindol (DAPI; cat# D1306, Thermo Fisher Scientific Inc.) in 1x TBS, then washed once again with 1x TBS. Imaging was performed with an Opera HCA reader (PerkinElmer) using a 405 nm and a 561 nm laser.

Crystallisation and data collection

Crystallisation and data collection were carried out as described in the Supplement.

Structure solution and refinement

Structure solution and refinement were carried out as described in the Supplement.

Data analysis

Data analysis was carried out as described in the Supplement.

Results

Selectivity of AB2 and AB20 for TrkB isoforms

The selectivity of AB2 and AB20 was analyzed in three CHO cell lines that recombinantly overexpressed TrkA, TrkB or TrkC. The response of the three cell lines was measured using the Alpha^{TM} format. This Alpha^{TM} assay quantified the phosphorylation of a homologous tyrosine (corresponding to Tyr706 of TrkB) in the cytoplasmic domain of all three Trk isoforms. While NGF and NT3, physiological agonists of TrkA and TrkC, respectively, induced the efficient phosphorylation of the respective tyrosine in their cognate receptors, neither AB2 nor AB20 produced any detectable pTrkA or pTrkC (Fig. 1A, C). In contrast, both AB2 and AB20 generated a clear phosphorylation of Tyr706 in the TrkB overexpressing CHO cells (Fig. 1B). Hereby, AB2 displayed a similar molar potency as BDNF, and AB20 a significantly weaker molar potency than BDNF (Table 1; Supplemental Figure 1). The maximal extent of TrkB phosphorylation after AB2 or AB20 administration was, however, significantly below the amount of pTrkB after maximal BDNF stimulation (Table 1; Supplemental Figure 1). The finding of TrkB selectivity for AB2 and AB20 was further corroborated by an immunofluorescence study, in which the same two antibodies only detected epitopes in the TrkB-overexpressing but not in the TrkA- or TrkC-overexpressing CHO cells (Fig. 1D). Selective TrkB activation was also reflected by an orthogonal Western Blot analysis (Supplemental Figure 2).

Transcriptional modulation by BDNF, AB2 and AB20

NGS was employed to monitor how BDNF, AB2 and AB20 modulate the transcriptome of the hiPS cell-derived GRINCH neurons. In this study, 42 genes were

JPET Fast Forward. Published on March 28, 2017 as DOI: 10.1124/jpet.117.240184
This article has not been copyedited and formatted. The final version may differ from this version.

selected as described in the Supplement. Briefly, the selection was based upon (i) the absolute gene expression levels after BDNF, AB2, AB20 or control IgG stimulation, (ii) the degree of deregulation after agonist treatment, and (iii) the False Discovery Rate (FDR).

Among these 42 genes, all 29 genes that were upregulated by BDNF were also upregulated by AB2 and by AB20 (Fig. 2A). Likewise, all 13 genes that were downregulated by BDNF were also downregulated by AB2 and AB20. Hereby the rank-order of the fold changes was very similar between BDNF versus control and AB2 versus control, as well as between BDNF versus control and AB20 control. *VGF*, for instance, was the most upregulated gene for all three agonists. However, the amplitude of deregulation for several genes was higher for BDNF than for AB2 or AB20, for example in regard to the upregulated genes *BCL2L2PABPN*, *HES4*, and *RELL2* as well as the downregulated genes *ANXA1P2* and *RP11466H18*.1 (Fig. 2A). In contrast, the amplitude of deregulation was very similar between AB2 and AB20 (Fig. 2B).

In accordance with the above described overlap of downstream signaling between BDNF and the two agonistic antibodies, the 24 genes that were at least twofold deregulated by AB2 are a true subset of the 41 genes that were at least twofold deregulated by BDNF (Fig. 2C). Likewise, 21 of the 22 genes that were at least twofold deregulated by AB20 are a subset of the 41 genes that were at least twofold deregulated by BDNF. In summary, AB2 and AB20 deregulated an overlapping gene set with BDNF, but BDNF acted as a more efficacious agonist than the two antibodies in regard to the amplitude of deregulation.

Modulation of TrkB signaling pathways by BDNF, AB2 and AB20

The stimulation of endogenous TrkB signaling by BDNF, AB2 and AB20 was measured using GRINCH neurons as model cells. Downstream signaling (Minichiello, 2009) was monitored with a focus on phosphorylation of ERK, AKT and CREB, as well as on the expression of *VGF* (Fig. 3A), an early response gene after neurotrophin receptor activation (Alder et al., 2003). In the pTrkB Alpha™ assay (Fig. 3B), BDNF, AB2 and AB20 displayed EC_{50} values (Table 1) of 0.67 ng/mL (25 pM), 10 ng/mL (67 pM) and 80 ng/mL (530 pM). Thus, all three agonists were significantly more potent in regard to the GRINCH neurons than to the TrkB overexpressing CHO (CHO-TrkB) cells (Table 1). Hereby, AB2 and AB20 were pronouncedly less efficacious in respect of TrkB phosphorylation than the physiological agonist BDNF in both cell types: Both antibodies produced an approximately 30% maximal stimulation (normalized to the maximal stimulation by BDNF as 100 %) in the CHO-TrkB cells and approximately half-maximal stimulation in the GRINCH neurons (Table 1).

To explore the downstream efficacies of the TrkB agonists, Alpha™ assays were adapted to the GRINCH neurons, which selectively detected the phosphorylation of ERK, of AKT, and of CREB (Minichiello, 2009). In the assay for phosphorylated ERK (pERK; Fig. 3C), BDNF, AB2 and AB20 displayed potencies (Table 1) that were 2-3 fold higher than with respect to phosphorylation of TrkB in the same cells. However, the rank-order of potencies for the three agonists was the same between the pTrkB and the pERK signal, with BDNF > AB2 > AB20. The relative efficacies for ERK phosphorylation of AB2 and AB20 were found to be 79 % and 72 %, in comparison to relative efficacies of 51 % and 46 %, respectively, for the above described TrkB phosphorylation (Table 1).

JPET Fast Forward. Published on March 28, 2017 as DOI: 10.1124/jpet.117.240184
This article has not been copyedited and formatted. The final version may differ from this version.

Potencies of all three agonists in the assay for phosphorylated AKT (pAKT) assay (Table 1; Fig. 3D) were very similar to the potencies in the pERK assay, thereby maintaining also the same rank-order of potencies as in the pTrkB assay. In regard to AKT phosphorylation, however, AB2 and AB20 were found to be about equally efficacious agonists as BDNF (Table 1; Fig. 3D). The absolute potencies of the three agonists in regard to the signals for phosphorylated CREB (pCREB) were similar to the respective potencies for the above described phosphorylation events (Table 1; Fig. 3E). Moreover, the rank-order of potencies among the three TrkB agonists was once more maintained. Similar to the observations for the pAKT signal, AB2 displayed a comparable efficacy as BDNF in respect of CREB phosphorylation. As to AB20, this antibody even exceeded the efficacy of the physiological agonist BDNF by a factor of approximately 1.8.

Finally, the effect of the three agonists was investigated in the context of a TrkB-induced transcription event. As described above for the NGS experiments (Fig. 2), the most extensive increase of transcription after TrkB activation was observed in regard to the *VGF* gene. In consequence, the agonist induced expression of the *VGF* gene was monitored in GRINCH neurons using an RT-PCR assay (Fig. 3F). In line with all four above described TrkB-modulated phosphorylation events, the three TrkB agonists stimulated *VGF* transcription with picomolar potencies and with the same rank-order of potencies. Similar to AKT phosphorylation, the efficacies of AB2 and AB20 were comparable to that of the physiological agonist BDNF.

The pan-Trk kinase domain inhibitor K252a (Massa et al., 2010) inhibited all five above described agonist-stimulated signaling events (Supplemental Figure 3), endorsing the view that all observed agonistic effects are mediated by the Trk receptor. In further agreement with previously described TrkB modulated signaling

JPET Fast Forward. Published on March 28, 2017 as DOI: 10.1124/jpet.117.240184
This article has not been copyedited and formatted. The final version may differ from this version.

routes (Massa et al., 2010), (i) the mitogen-activated protein kinase kinase (MKK) inhibitor PD98059 partially inhibited ERK phosphorylation, (ii) the phosphatidylinositol 3 (PI 3)-kinase inhibitor LY294002 decreased AKT phosphorylation, and (iii) the phospholipase C (PLC) inhibitor U73122 reduced phosphorylation of CREB for all three agonists (Supplemental Figure 3).

Allosteric binding mode of AB20

BDNF binding to the TrkB immunoglobulin superfamily d5 domain was modeled upon the previously published structures of (i) the TrkB-d5 domain in complex with NT4/5 (Banfield et al., 2001) and of (ii) the unliganded form of BDNF in a heterodimer with NT4 (Robinson et al., 1999). The validity of the TrkB-d5/BDNF model was further corroborated by the complex structure of the TrkA-d5 domain with NGF, which displayed homologous interaction sites between the neurotrophin and the receptor surface as observed for the complex between TrkB-d5 and NT4/5 (Banfield et al., 2001). Furthermore, affinity studies carried out between the Trk-d5 fragment and NT4/5 or BDNF had suggested that the neurotrophin binding site is wholly located within the d5 domain.

While AB2 was known to act orthosterically with BDNF (Lin et al., 2010), AB20 was assumed to bind to a distinct epitope outside of the BDNF-binding site (Wang et al., 2010). Indeed, the described x-ray crystallography studies identified a complex structure of the BDNF-binding TrkB-d5 domain and AB20 (Fig. 4) with the binding epitope of AB20 localized at β-strands C, F, and G, on the opposite side of the TrkB-d5 domain with respect to the BDNF binding site.

JPET Fast Forward. Published on March 28, 2017 as DOI: 10.1124/jpet.117.240184
This article has not been copyedited and formatted. The final version may differ from this version.

Synergies between BDNF and AB2 or AB20

In order to validate whether AB2 or AB20 exerted a synergistic effect with BDNF or with each other, a series of co-stimulation studies in the Alpha™ was carried out using the GRINCH neurons as model cells. When AB2 was administered together with BDNF, maximal BDNF-driven phosphorylation of TrkB was reduced at high concentrations of AB2 (Fig. 5A). This observation is in accordance with the above described competitive binding mode between BDNF and AB2 in regard to TrkB. In contrast to AB2, high concentrations of AB20 did not reduce the BDNF-driven phosphorylation of TrkB. However, there was also no synergistic or additive effect between BDNF and AB20 in regard to maximal stimulation – even at high AB20 concentrations (Fig. 5B). Likewise the EC_{50} value for the BDNF stimulation was not significantly altered by the presence of AB20.

As described above, AB2 and AB20 acted as partial agonists in regard to TrkB phosphorylation when applied individually (Table 1). In a co-stimulation experiment with both TrkB-directed antibodies, an additive effect was observed in regard to the maximal pTrkB signal (Fig. 5C). At the highest concentrations of both AB2 and AB20, the attained pTrkB signal was similar to the maximal stimulation obtained with BDNF. In regard to potency values, there was no significant synergistic effect between AB2 and AB20.

Kinetics of TrkB signaling pathways after stimulation with BDNF, AB2 or AB20

Using the above described Alpha™ formats as read-outs, three different stimulation schemes (Fig. 6A) were applied in order to analyze how BDNF, AB2 and AB20 regulate the phosphorylation of TrkB, ERK, AKT, and CREB, kinetically. For

JPET Fast Forward. Published on March 28, 2017 as DOI: 10.1124/jpet.117.240184
This article has not been copyedited and formatted. The final version may differ from this version.

scheme I, referred to as “re-stimulation”, the indicated agonist was administered for a pulse period of 15 min, then washed off and re-administered for a second pulse of 15 min at the end of the indicated time period. Using this scheme, the phosphorylation of TrkB as well as of its downstream effectors ERK, AKT and CREB could only be re-stimulated by AB20 (Fig. 6B).

For scheme II, referred to as “single pulse stimulation”, the indicated agonist was administered for a pulse period of 15 min, washed off and then omitted from the cell supernatant for the remainder of the indicated time period. In the first 6.5 h after “single pulse stimulation”, the BDNF-stimulated Alpha^{TM} signals for pTrkB, pERK, and pAKT maintained a higher level than the respective AB2- or AB20-stimulated signals (Fig. 6C). In the same timeframe, the AB2-stimulated Alpha^{TM} signals for pTrkB, pERK, and pAKT were higher than the respective AB20-stimulated signals. In regard to pCREB signal kinetics, there were hardly any differences between stimulation by BDNF or AB2. However, the level of pCREB generated by AB20 was lower than that generated by BDNF or AB2 during 2.5 h after the single pulse stimulation.

For scheme III, referred to as “continuous stimulation”, the specified agonist was administered at the beginning, then remained in the cell supernatant for the remainder of the indicated time period. For time-periods of up to two h, the BDNF-stimulated Alpha^{TM} signals for pTrkB, pERK and pAKT were higher than the respective signals with AB2 or AB20 stimulation (Fig. 6D). Only in regard to the pCREB signal, the AB20 stimulation provided higher Alpha^{TM} signals than BDNF or AB2 for all analyzed incubation periods.

Discussion

The purpose of this work was to characterize two TrkB-directed antibodies, AB2 and AB20, in terms of pharmacology and downstream signaling using the physiologically relevant GRINCH neurons as a cellular model.

The binding selectivity of AB2 and AB20 for the TrkB isoform was supported by immunofluorescence investigation, where both antibodies immune-stained the TrkB-overexpressing but not the TrkA- or TrkC-overexpressing CHO cells. Likewise, a functional selectivity of these two antibodies was observed using the same three CHO cell lines recombinantly overexpressing one of the Trk receptors: NGF and NT3, the physiological agonists of TrkA and TrkC, respectively, stimulated Trk phosphorylation in CHO cells that were transfected with TrkA or TrkC, respectively. But neither AB2 nor AB20 was capable of inducing Trk activation in the latter two cell lines. In contrast, both AB2 and AB20 were capable of functionally activating Trk phosphorylation in the CHO cells that overexpressed TrkB. However, the maximal extent of AB2- or AB20-driven phosphorylation of TrkB was significantly below the efficacy of the BDNF-driven response both in the TrkB-overexpressing CHO cells and in the GRINCH neurons.

Similar to the dimeric physiological agonist BDNF, both TrkB-directed antibodies are supposed to be capable of inducing TrkB receptor dimerization (Cazorla et al., 2011). BDNF may, however, lead to a functionally preferred dimer arrangement that is more conducive to, for instance, receptor transphosphorylation (Cazorla et al., 2011). Concerning AB20 the latter hypothesis was corroborated by the here described x-ray structure where this antibody binds TrkB on the opposite site of the TrkBd5 domain when compared to the presumable BDNF binding site. Yet, also for AB2, for which the binding site on TrkB overlaps with that of BDNF, the steric relationship and

Euclidean distance of the two TrkB protomers may be quite different from the BDNF-induced physiological receptor dimerization.

Apart from presumably rendering the TrkB dimer less suitable for transphosphorylation, the AB2- or AB20-induced spatial relationship of the TrkB protomers may modulate the accessibility of the intracellular phosphorylation sites in regard to further kinases that accept TrkB as a substrate (Huang and McNamara, 2010). Accordingly, such different agonist-dependent TrkB-dimeric structures may also result in diversely efficacious downstream signaling. This could explain why AB2 and AB20 displayed lower efficacies than BDNF also in regard to TrkB-modulated ERK phosphorylation, and why AB20 appeared to be more efficacious than BDNF or AB2 in respect of CREB phosphorylation. Notably, a similar partial agonism of some commercially available TrkB-directed antibodies when compared to BDNF as a full agonist had been observed previously (Cazorla et al., 2011). The partial efficacy of AB2 and AB20 in comparison to BDNF was also reflected by NGS experiments where the amplitude of deregulation for the majority of the monitored genes was higher for BDNF than for the two agonistic antibodies.

In the work of Todd et al. (Todd et al., 2014), the signaling efficacies of two different TrkB-agonistic antibodies were found to be similar to BDNF after a 5 h incubation period. Likewise, Qian et al. (Qian et al., 2006) established five TrkB-directed antibodies that all stimulated TrkB-dependent luciferase signaling after an incubation time of 16 h to a similar extent as BDNF. Correspondingly, AB2 and AB20 in this work displayed similar efficacies as BDNF for example in the *VGF* transcription read-out after a 6 h incubation period. Hereby, the signal accumulation over the incubation period of several hours may mask a partial agonism of an antibody as observed for the respective phosphorylation measurements after incubation periods of 15 min.

JPET Fast Forward. Published on March 28, 2017 as DOI: 10.1124/jpet.117.240184
This article has not been copyedited and formatted. The final version may differ from this version.

Additionally, AB2 and AB20 displayed similar maximal effects as BDNF with respect to AKT phosphorylation despite the agonist incubation time of 15 min. In order to explain this finding one needs to consider that for some of the downstream TrkB-dependent signaling events other upstream members of the signaling chain might constitute the bottleneck of efficacy. In consequence, a more efficacious pTrkB stimulation by BDNF than by AB2 or AB20 will not necessarily translate into a higher downstream readout. In agreement with this view, a broad overlap of the deregulated gene sets induced by any of the three here investigated agonists was observed in the NGS experiments. These observations argue against highly divergent ligand-biased signaling routes between BDNF, AB2 and AB20. In summary, the therapeutic value of an antibody with increased efficacy in respect to an upstream signaling event will depend on the translation of this efficacy into disease-relevant downstream events. For instance, AB2 and AB20 were found to drive the expression of the synaptic plasticity marker activity-regulated cytoskeleton-associated protein (ARC) with a to some extent lower efficacy than BDNF in rat primary neurons (Supplemental Figure 4). *Arc* is an immediate-early gene, transcribed in response to neuronal activation. The newly translated protein is believed to play a critical role in learning and memory-related molecular processes (McIntyre et al., 2005). In GRINCH neurons, an administration of BDNF, AB2, or AB20 over 7 d produced an approximately 2.5-3 fold increase of the *VGF* mRNA level without any significant efficacy differences between the three agonists (Supplemental Figure 5).

The x-ray structure with the AB20-binding epitope on the opposite side of the d5 domain compared to the BDNF or AB2 binding site held out the prospect of synergistic TrkB activation. Indeed, AB2 and AB20 displayed additive effects on TrkB phosphorylation in GRINCH neurons. However, the maximal effect of the co-

JPET Fast Forward. Published on March 28, 2017 as DOI: 10.1124/jpet.117.240184
This article has not been copyedited and formatted. The final version may differ from this version.

stimulation with both TrkB-directed antibodies did not exceed the maximal pTrkB signal as attained after solely stimulating with BDNF.

In contrast to the additive effects observed between AB2 and AB20, no significant synergism in regard to the pTrkB signal was observed in a co-stimulation approach with AB20 and BDNF using the same model cells. One explanation for this finding might be that the more potently induced BDNF-driven TrkB activation leads to a receptor dimer that is spatially incompatible with the AB20-induced dimer. In consequence, BDNF dominates the pTrkB effect in co-stimulation experiments with AB20. Finally, the BDNF-stimulated phosphorylation of TrkB was inhibited at high concentrations of AB2, which is in good agreement with the supposedly overlapping binding sites of BDNF and AB2.

A “re-stimulation” approach was carried out on the GRINCH neurons with two fifteen-minute pulses of agonist administration, the first one prior to and the second one after a gap period without agonist in the cell supernatant. With increasing length of the agonist-free intermittent period, the BDNF- or AB2-driven Alpha^{TM} signals for pTrkB, pERK, pAKT and pCREB declined. Only AB20 led to an increased or at least maintained signal in all four phosphorylation assays after longer agonist-free gap periods. One possible explanation is that both BDNF and AB2 caused receptor internalization, whereas AB20 might have stimulated the phosphorylation of TrkB and downstream signaling without downregulating the receptor from the cell surface. If the receptor remains at the plasma membrane the extracellular agonist may dissociate into the cell supernatant in the intermittent periods, thereby unblocking the ligand binding site of TrkB for a renewed stimulation during the second agonist pulse.

Such an explanation is in concord with results of the “single pulse stimulation” experiments, where the decline of pTrkB, pERK, pAKT and pCREB was most

pronounced after AB20 stimulation: If TrkB remains at the plasma membrane, AB20 may dissociate into the agonist-free supernatant and thereby diminish the activation state of the receptor. The above working hypothesis is also in agreement with the findings in the “continuous stimulation” experiment: If TrkB-dissociated AB20 may be replenished from the cell medium during the whole course of the experiment, the signal decrease during continuous AB20 administration should be similar to the signal decline during permanent AB2 exposure. Indeed, the Alpha^{TM} signals between AB20 and AB2 in respect of pTrkB, pERK and pAKT were virtually identical in the “continuous stimulation” mode. In regard to CREB phosphorylation, the Alpha^{TM} signal stimulated by AB20 was even higher than that induced by BDNF or AB2 for all observed time-points. In all here described kinetic experiments, the contribution of a potential agonist-stimulated novel synthesis in regard to TrkB, ERK, AKT and CREB cannot be estimated. Accordingly, the measured concentrations of phosphorylated signaling proteins cannot be recalculated into a relative value of “percent phosphorylation”.

The employment of GRINCH neurons as model cells for the pharmacological studies provided several benefits. Thus, transcriptional and immunofluorescence-based analysis showed these hiPS-derived cells to be a balanced mixture of various neuronal subtypes including particular cortical neurons, the latter cells being of particular relevance to study disease-relevant TrkB pharmacology (Traub et al., 2017). Practically, the use of these model cells profited from the option to transiently freeze their neural precursor cells, from which the GRINCH neurons can be derived by a small molecule-accelerated, two week neuronal differentiation protocol.

Pharmacological modulation of TrkB holds out the prospect of addressing various neurological diseases. In this work, two previously described TrkB-agonistic

antibodies were compared to BDNF activity in terms of TrkB receptor selectivity, potency, and efficacy. Both antibodies were found to be TrkB isoform selective. Both AB2 and AB20 displayed potencies in the picomolar range in regard to the various above described pharmacological readouts. In regard to some of the TrkB-modulated signaling events, neither AB2 nor AB20 attained the same maximal effect as the physiological agonist BDNF. If this partial agonism of the antibodies translates into an attenuated *in vivo* therapeutic effect, the respective cellular assay formats will be important tools for further optimization of the drug candidates. Likewise, the *in vitro* observed differences in re-stimulation kinetics may turn out to be predictive for *in vivo* tachyphylactic drug effects. As antibodies generally cross the BBB only to a limited extent, an appropriate trans-BBB shuttle system (Pardridge, 2012) may be required to render AB2 and AB20 valuable therapeutic tools for CNS disorders in the future. In summary, the above developed techniques of pharmacological analysis together with the GRINCH neurons open new experimental routes of tremendous potential for early TrkB-directed drug discovery.

Acknowledgments

We thank Dirk Stenkamp, Daniel Bischoff, Ulrike Küfner-Mühl, Martin John Valler, Marcel Leist, Robert Ries, Tobias Hildebrand, German Leparc, Stefan Jäger, Natascha Piede, Michael Sulger, Achim Lietz, Anita Bloching, Margit Bauer, Kristina Vogel, Sebastian Bandholtz, Rolf Herrmann.

Authorship Contributions

Participated in research design: Traub, Rosenbrock, Hospach, Hörer, Heilker

Conducted experiments: Traub, Hospach

Contributed new reagents or analytic tools: Stahl, Florin

Performed data analysis: Simon

Wrote or contributed to the writing of the manuscript: Traub, Stahl, Rosenbrock, Simon, Florin, Hörer, Heilker

References

Adachi N, Numakawa T, Richards M, Nakajima S and Kunugi H (2014) New insight in expression, transport, and secretion of brain-derived neurotrophic factor: Implications in brain-related diseases. *World J Biol Chem* **5**:409-428.

Alder J, Thakker-Varia S, Bangasser DA, Kuroiwa M, Plummer MR, Shors TJ and Black IB (2003) Brain-derived neurotrophic factor-induced gene expression reveals novel actions of VGF in hippocampal synaptic plasticity. *J Neurosci* **23**:10800-10808.

Banfield MJ, Naylor RL, Robertson AG, Allen SJ, Dawbarn D and Brady RL (2001) Specificity in Trk receptor:neurotrophin interactions: the crystal structure of TrkB-d5 in complex with neurotrophin-4/5. *Structure* **9**:1191-1199.

Barde YA, Edgar D and Thoenen H (1982) Purification of a new neurotrophic factor from mammalian brain. *EMBO J* **1**:549-553.

Bothwell M (2014) NGF, BDNF, NT3, and NT4. *Handb Exp Pharmacol* **220**:3-15.

Cauchon E, Liu S, Percival MD, Rowland SE, Xu D, Binkert C, Strickner P and Falgueyret JP (2009) Development of a homogeneous immunoassay for the detection of angiotensin I in plasma using AlphaLISA acceptor beads technology. *Anal Biochem* **388**:134-139.

Cazorla M, Arrang JM and Premont J (2011) Pharmacological characterization of six trkB antibodies reveals a novel class of functional agents for the study of the BDNF receptor. *Br J Pharmacol* **162**:947-960.

Heilker R, Traub S, Reinhardt P, Scholer HR and Sterneckert J (2014) iPS cell derived neuronal cells for drug discovery. *Trends Pharmacol Sci* **35**:510-519.

Huang YZ and McNamara JO (2010) Mutual regulation of Src family kinases and the neurotrophin receptor TrkB. *J Biol Chem* **285**:8207-8217.

Lin CY, Chaparro Riggers JF, Grishanin RN, Stratton JR and Zhai W (2010) Agonist anti-TrkB monoclonal antibodies. PCT filed: Feb. 1, 2010, in *US20100196390A1*.

Longo FM and Massa SM (2013) Small-molecule modulation of neurotrophin receptors: a strategy for the treatment of neurological disease. *Nat Rev Drug Discov* **12**:507-525.

Massa SM, Yang T, Xie Y, Shi J, Bilgen M, Joyce JN, Nehama D, Rajadas J and Longo FM (2010) Small molecule BDNF mimetics activate TrkB signaling and prevent neuronal degeneration in rodents. *J Clin Invest* **120**:1774-1785.

McIntyre CK, Miyashita T, Setlow B, Marjon KD, Steward O, Guzowski JF and McGaugh JL (2005) Memory-influencing intra-basolateral amygdala drug infusions modulate expression of Arc protein in the hippocampus. *Proc Natl Acad Sci U S A* **102**:10718-10723.

Minichiello L (2009) TrkB signalling pathways in LTP and learning. *Nat Rev Neurosci* **10**:850-860.

Pardridge WM (2012) Drug transport across the blood-brain barrier. *J Cereb Blood Flow Metab* **32**:1959-1972.

Qian MD, Zhang J, Tan XY, Wood A, Gill D and Cho S (2006) Novel agonist monoclonal antibodies activate TrkB receptors and demonstrate potent neurotrophic activities. *J Neurosci* **26**:9394-9403.

Robinson RC, Radziejewski C, Spraggon G, Greenwald J, Kostura MR, Burtnick LD, Stuart DI, Choe S and Jones EY (1999) The structures of the neurotrophin 4 homodimer and the brain-derived neurotrophic factor/neurotrophin 4 heterodimer reveal a common Trk-binding site. *Protein Sci* **8**:2589-2597.

Shi Y, Kirwan P and Livesey FJ (2012) Directed differentiation of human pluripotent stem cells to cerebral cortex neurons and neural networks. *Nat Protoc* **7**:1836-1846.

Todd D, Gowers I, Dowler SJ, Wall MD, McAllister G, Fischer DF, Dijkstra S, Fratantoni SA, van de Bospoort R, Veenman-Koepke J, Flynn G, Arjomand J, Dominguez C, Munoz-Sanjuan I, Wityak J and Bard JA (2014) A monoclonal antibody TrkB receptor agonist as a potential therapeutic for Huntington's disease. *PLoS One* **9**:e87923.

Traub S, Stahl H, Rosenbrock H, Simon E and Heilker R (2017) Upscaling of hiPS Cell-Derived Neurons for High-Throughput Screening. *SLAS Discov* **22**:274-286.

Wang Y, Cohen SB and Nasoff M (2010) Agonist TrkB antibodies and uses thereof. PCT filed: Nov. 6, 2007, in *US20100150914A1*.

Xu D, Alegre ML, Varga SS, Rothermel AL, Collins AM, Pulito VL, Hanna LS, Dolan KP, Parren PW, Bluestone JA, Jolliffe LK and Zivin RA (2000) In vitro characterization of five humanized OKT3 effector function variant antibodies. *Cell Immunol* **200**:16-26.

JPET Fast Forward. Published on March 28, 2017 as DOI: 10.1124/jpet.117.240184
This article has not been copyedited and formatted. The final version may differ from this version.

Legends for Figures

Fig. 1. Isoform selectivity of TrkB-directed antibodies AB2 and AB20. Dose response testing was carried out in three CHO cell lines, recombinantly overexpressing (A) TrkA, (B) TrkB, and (C) TrkC. The cells were stimulated with AB2, AB20 or control IgG. As positive controls, the physiological agonists NGF, BDNF, or NT-3 of the respective Trk isoforms were employed. Potency and efficacy values for (B) are given in Table 1. *N* = 8 replicates, error bars represent SEM. (D) Immune staining using AB2 and AB20 as primary antibodies was done on the same three cell lines: antibodies labeled in green, nuclear stain shown in white. Scale bar: 25 µM.

Fig. 2. Transcriptional modulation by BDNF, AB2, AB20 and IgG control in GRINCH neurons, analyzed by NGS. (A) 42 genes deregulated by BDNF, AB2 or AB20 versus IgG control. The amplitude of deregulation is indicated by the Log2R value. Red-coded numbers denote an upregulation, green-coded numbers a downregulation of gene expression. (B) Log2R values of the 42 genes deregulated by AB20 plotted versus the respective values for AB2. (C) Venn diagram. The numbers in the respective intersections designate the overlapping deregulated genes between the three agonists BDNF (green), AB2 (red) and AB20 (yellow). Red numbers designate upregulated genes, green numbers downregulated and black numbers the sum of deregulated genes. *N* = 4 replicates.

Fig. 3. TrkB-modulated signaling pathways in GRINCH neurons. (A) Dimeric BDNF stimulates TrkB dimerization. TrkB transphosphorylation leads to (i) activation of AKT via PI3K and PDK1, (ii) activation of Ras, MEK and ERK, (iii) activation of CREB

JPET Fast Forward. Published on March 28, 2017 as DOI: 10.1124/jpet.117.240184
This article has not been copyedited and formatted. The final version may differ from this version.

via activation of PLC, IP3 and CAMK, (iv) transcription activation of *VGF*. The agonist-modulated effects on phosphorylation are indicated by the measured Alpha™ values for (B) pTrkB, (C) pERK, (D) pAKT, and (E) pCREB. (F) RT-PCR data for the agonist-modulated effect on *VGF* expression based upon 2^(-ΔCP) values were normalized to vehicle-stimulated effects. Potency and efficacy values for (B-F) are given in Table 1. *N* = 4 replicates, error bars represent SEM.

Fig. 4. Binding sites of BDNF/NT4 and AB20 on TrkB-d5 domain. The complex structure of the TrkB-d5 domain with AB20 was resolved by x-ray. The binding epitope of AB20 is labeled in pink. The binding site of BDNF (black) was modeled upon the previously resolved complex structure of the TrkB-d5 domain with NT4.

Fig. 5. Co-stimulation by pairs of TrkB agonists. GRINCH neurons were co-stimulated by (A) BDNF and AB2, (B) BDNF and AB20, as well as (C) AB2 and AB20. One of the two agonist concentrations is given on the x-axis, the second co-stimulatory agonist concentration is indicated by the symbol (with the respective decadic logarithm of the mass concentration [mg/mL] indicated in the legend; the "veh" curve represents the use of vehicle instead of second agonist). *N* = 6 replicates, error bars represent SEM.

Fig. 6. Kinetics of TrkB signaling pathways after stimulation with BDNF, AB2 or AB20. TrkB stimulation was carried out using one of three (A) agonist administration schemes I-III: filled arrows indicate time spans with agonist in the cell supernatant,

JPET Fast Forward. Published on March 28, 2017 as DOI: 10.1124/jpet.117.240184
This article has not been copyedited and formatted. The final version may differ from this version.

striped arrows indicate time periods after washing off the agonist from the cell supernatant. GRINCH neurons were stimulated following schemes I, II, or III in (B), (C), or (D), respectively. The agonist-modulated effects on phosphorylation are shown as the measured Alpha™ values for pTrkB, pERK, pAKT, and pCREB, as indicated. Alpha™ signals are normalized to vehicle control. *N* = 8 replicates, error bars represent SEM.

JPET Fast Forward. Published on March 28, 2017 as DOI: 10.1124/jpet.117.240184
This article has not been copyedited and formatted. The final version may differ from this version.

Table

		CHO-TrkB	GRINCH neurons				
		pTrkB	**pTrkB**	**pERK**	**pAKT**	**pCREB**	***VGF***
BDNF	EC50 (ng/mL)	15	0.67	0.20	0.33	0.13	0.41
	95% C.I. (ng/mL)	13;16	0.58;0.76	1.6;2.6	0.26;0.42	0.13;0.16	0.31;0.55
	EC50 (pM)	540	25	7.4	12	4.7	15
	Efficacy (%)	100*	100*	100*	100*	100*	100*
	SEM (%)	1.1	2.1	2.8	3.0	2.4	3.4
AB2	EC50 (ng/mL)	59	10	5.1	4.6	1.1	2.5
	95% C.I. (ng/mL)	50;68	7.0;15	3.9;6.7	2.8;7.8	0.58;1.9	2.1;2.9
	EC50 (pM)	390	67	34	31	7.0	17
	Efficacy (%)	28	51	79	102	108	101
	SEM (%)	1;9	4.7	4.3	7.3	7.3	2.5
AB20	EC50 (ng/mL)	404	80	43	37	67	11
	95% C.I. (ng/mL)	340;480	57;110	32;57	30;46	49;92	8.6;15
	EC50 (pM)	2700	530	290	250	450	73
	Efficacy (%)	32	46	72	91	182	113
	SEM (%)	2;5	7.0	3.7	2.6	3.0	5.1

Table 1. EC_{50} and relative efficacy values for BDNF, AB2 and AB20 in the indicated TrkB signaling assays and using the indicated model cells. The EC_{50} values of BDNF, AB2, and AB20 are given in ng/mL and in pM. The 95% confidence intervals (95% C.I.) of the EC_{50} values are indicated. Relative efficacy values and the respective SEM values are given in %, normalized to BDNF as a full agonist with 100 %, as indicated by the asterisk *. Assays in the CHO-TrkB cells and in the GRINCH neurons were carried out using N=8 and N=4 replicates, respectively.

JPET Fast Forward. Published on March 28, 2017 as DOI: 10.1124/jpet.117.240184
This article has not been copyedited and formatted. The final version may differ from this version.

Figures

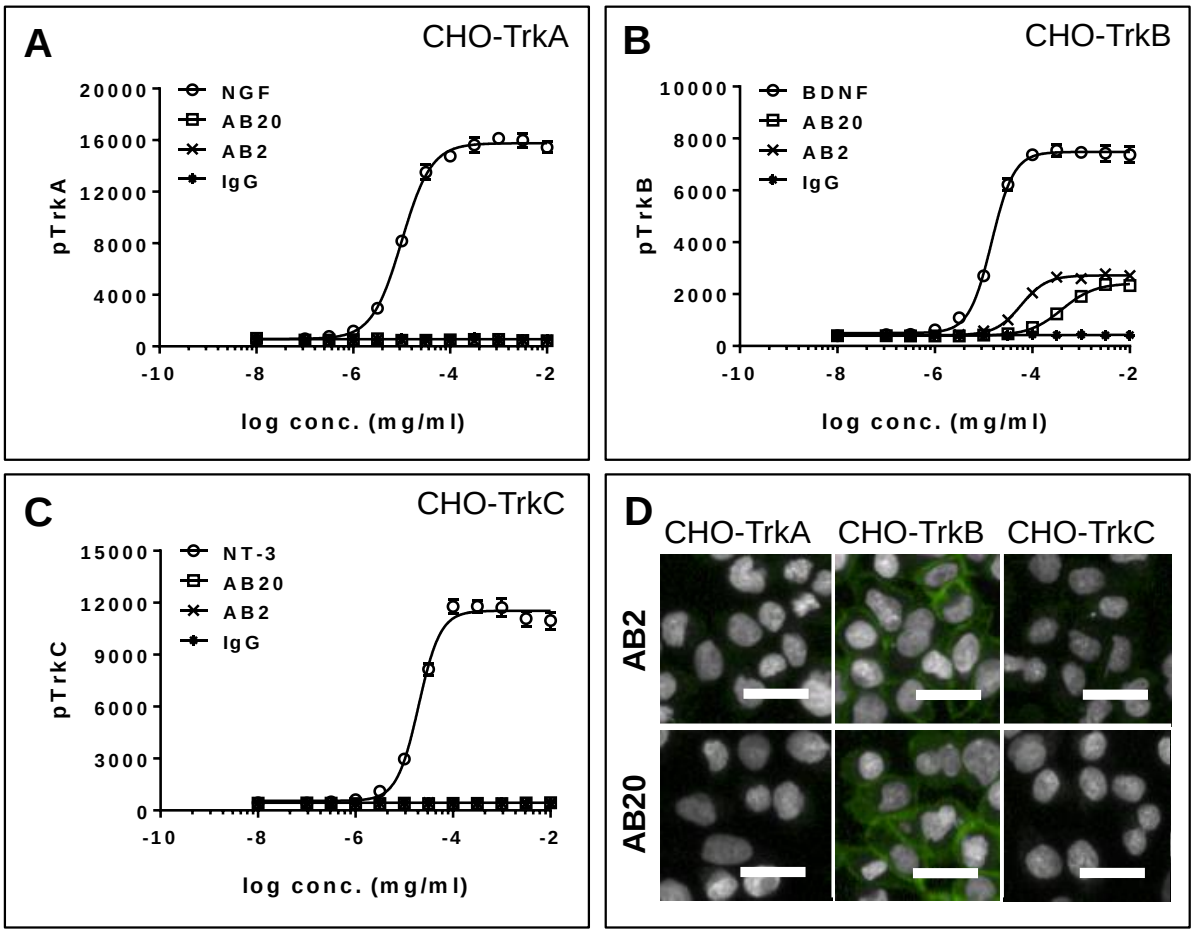

Figure 1

JPET Fast Forward. Published on March 28, 2017 as DOI: 10.1124/jpet.117.240184
This article has not been copyedited and formatted. The final version may differ from this version.

A

#	Gene Symbol	Log2R BDNF	Log2R AB2	Log2R AB20	Log2R IgG ctrl.
1	*VGF*	2.4	2.2	2.2	-0.1
2	*GPR50*	2.0	2.1	2.1	-0.2
3	*ETV4*	1.9	1.8	1.6	-0.2
4	*NPTX1*	1.5	1.3	1.3	-0.2
5	*ACHE*	1.5	1.2	1.2	-0.3
6	*PCSK1N*	1.4	1.1	0.9	-0.7
7	*HAP1*	1.4	1.2	0.9	-0.2
8	*PTPRN*	1.4	1.1	1.1	-0.2
9	*BCL2L2PABPN*	1.4	0.8	0.6	-0.5
10	*TH*	1.3	1.1	0.8	-0.3
11	*PDE18*	1.3	1.1	1.2	-0.1
12	*RP11465B22.3*	1.3	0.8	0.8	-0.1
13	*C19ORF26*	1.2	1.0	0.8	-0.3
14	*ANK1*	1.2	1.0	1.2	0.0
15	*SHC4*	1.2	1.3	1.2	-0.1
16	*HES4*	1.2	0.7	0.6	-0.5
17	*PPP1R16A*	1.2	0.9	0.7	-0.4
18	*BEGAIN*	1.1	1.0	0.9	-0.1
19	*RELL2*	1.1	0.7	0.6	-0.3
20	*CASKIN1*	1.1	0.9	0.7	-0.2
21	*C1ORF159*	1.1	0.6	0.6	-0.1
22	*ARHGDIG*	1.0	0.8	0.5	-0.3
23	*MIF*	1.0	0.7	0.6	-0.2
24	*RP11274B21.4*	1.0	0.7	0.6	0.1
25	*SCG2*	1.0	1.0	1.1	0.0
26	*SCAND1*	1.0	0.6	0.4	-0.3
27	*EXOSC5*	1.0	0.6	0.6	-0.4
28	*ATPSD*	1.0	0.7	0.5	-0.2
29	*LRRTM1*	0.9	1.0	1.0	-0.1
30	*RPL18AP3*	-1.0	-1.0	-0.9	0.0
31	*MORF4L1P1*	-1.1	-0.8	-1.0	-0.1
32	*RP11343H5.4*	-1.2	-1.1	-0.8	0.2
33	*RP1159A19.3*	-1.7	-1.0	-1.2	0.1
34	*RP11425L10.1*	-1.7	-1.1	-1.3	-0.3
35	*CTD2192J16.15*	-1.7	-1.6	-2.0	-0.1
36	*GS1257G1.1*	-1.8	-1.3	-1.4	-0.2
37	*RP1140C6.2*	-2.1	-1.8	-1.9	0.0
38	*RPL14P1*	-2.2	-1.7	-1.7	0.2
39	*PTGES3P1*	-2.9	-1.9	-1.9	0.1
40	*ANXA1P2*	-3.1	-1.6	-1.5	0.2
41	*UBA52P5*	-4.6	-3.8	-3.7	0.5
42	*RP11466H18.1*	-5.4	-3.1	-3.0	0.4

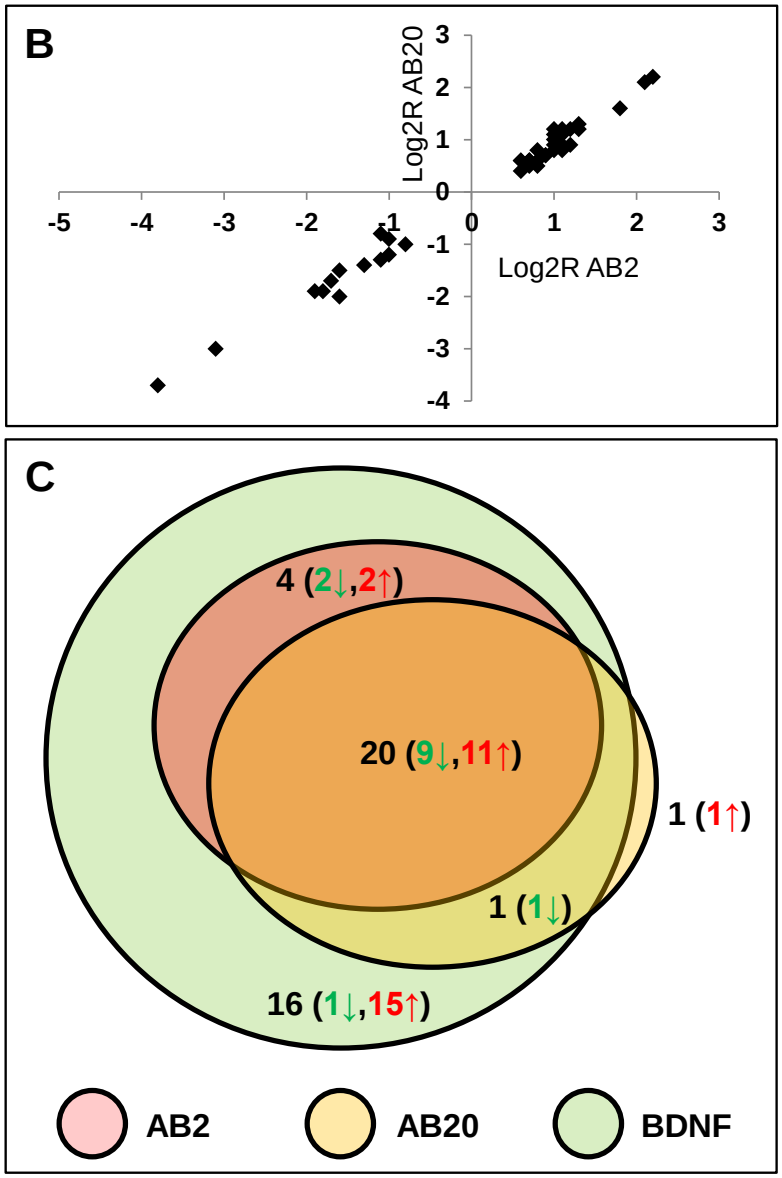

Figure 2

JPET Fast Forward. Published on March 28, 2017 as DOI: 10.1124/jpet.117.240184
This article has not been copyedited and formatted. The final version may differ from this version.

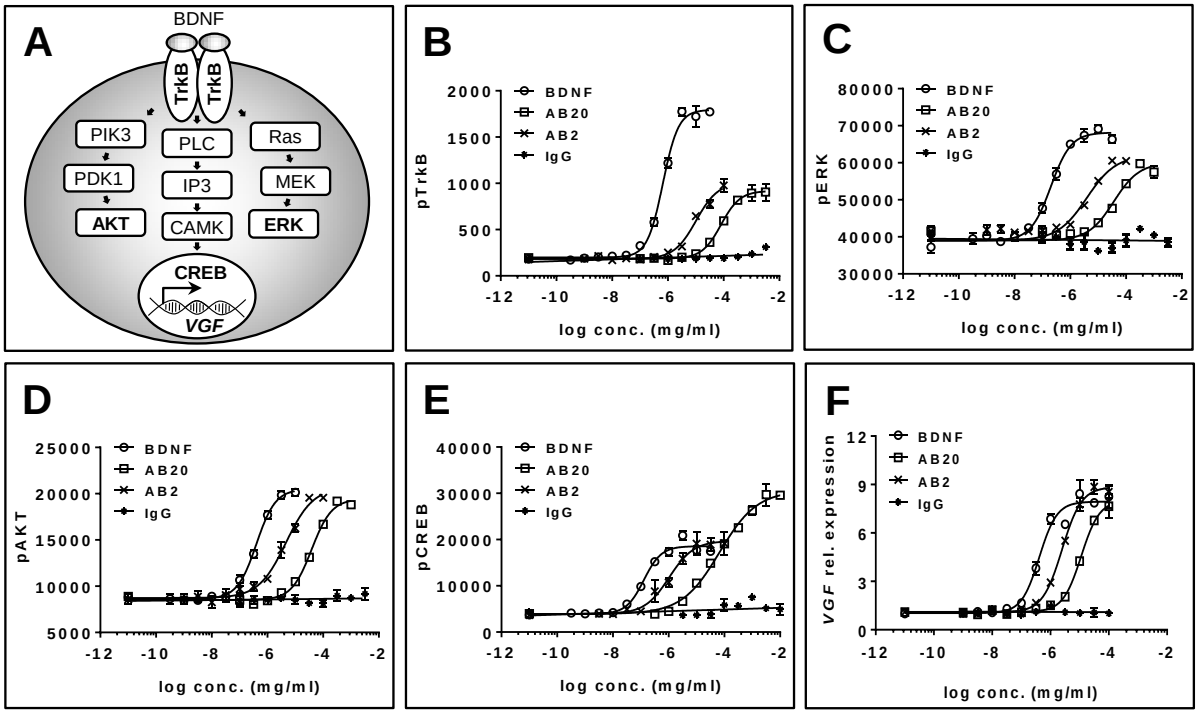

Figure 3

JPET Fast Forward. Published on March 28, 2017 as DOI: 10.1124/jpet.117.240184
This article has not been copyedited and formatted. The final version may differ from this version.

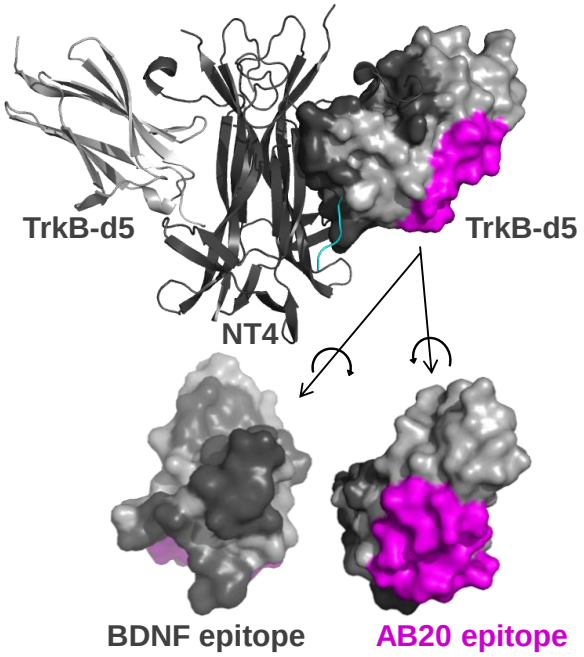

Figure 4

JPET Fast Forward. Published on March 28, 2017 as DOI: 10.1124/jpet.117.240184
This article has not been copyedited and formatted. The final version may differ from this version.

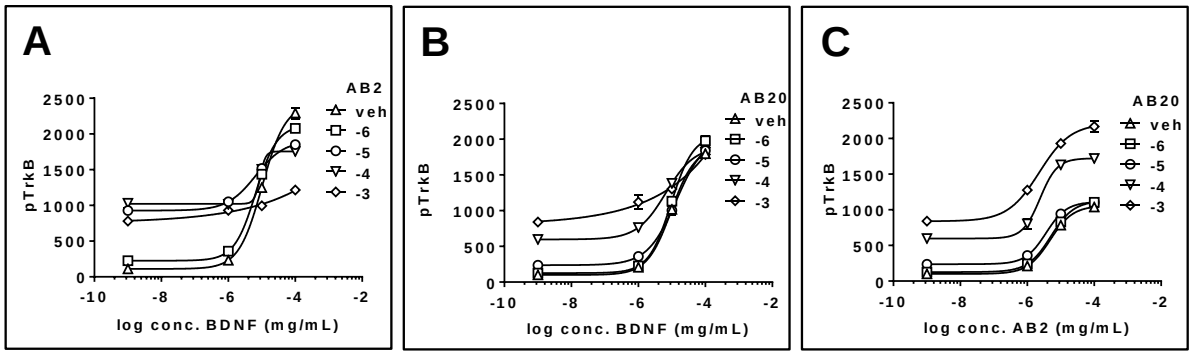

Figure 5

JPET Fast Forward. Published on March 28, 2017 as DOI: 10.1124/jpet.117.240184
This article has not been copyedited and formatted. The final version may differ from this version.

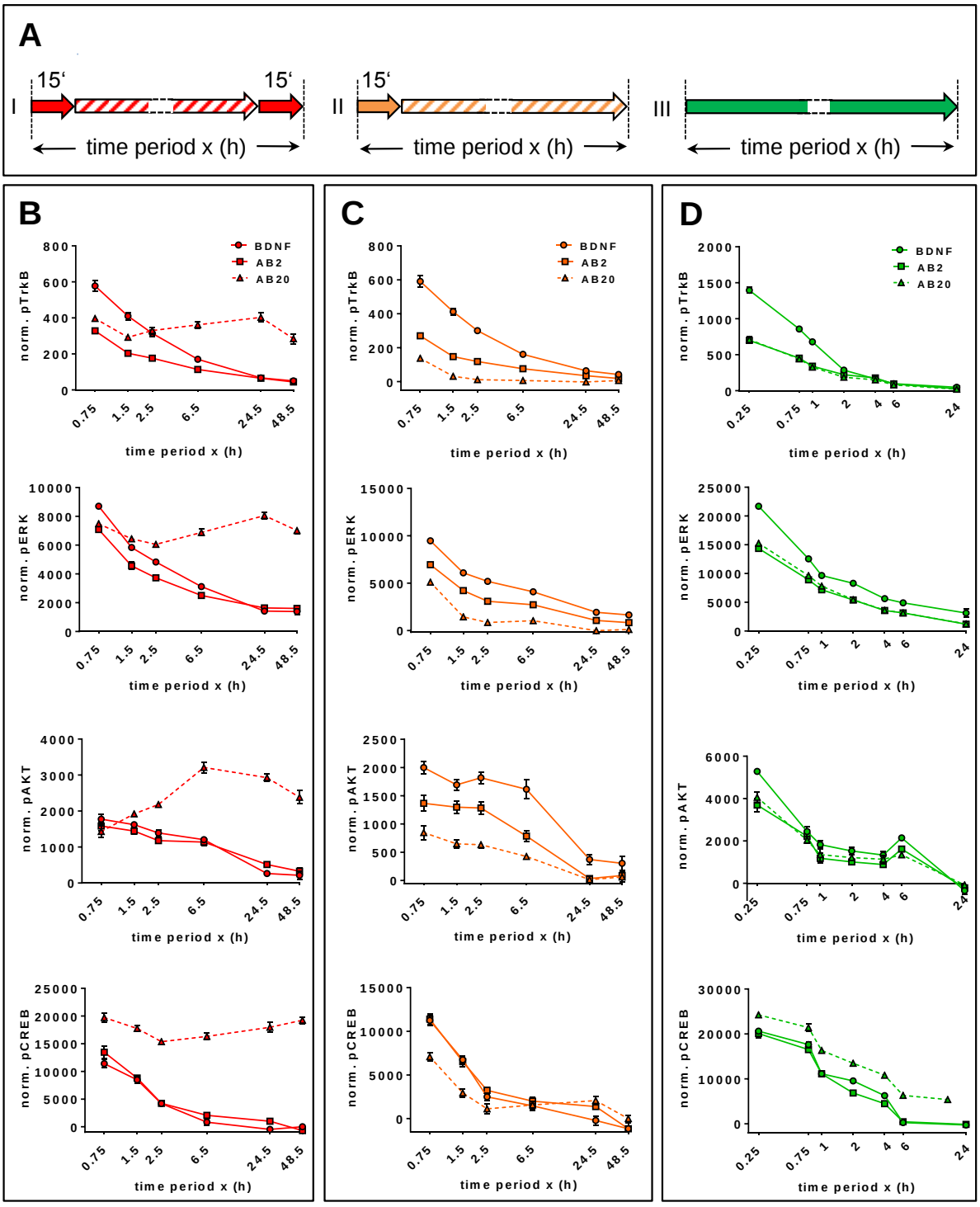

Figure 6